A New Approach on Optimization of the Rational Function Model of High-Resolution Satellite Imagery

Yongjun Zhang, Yihui Lu, Lei Wang, and Xu Huang

***Abstract*—Overparameterization is one of the major problems that the rational function model (RFM) faces. A new approach of RFM parameter optimization is proposed in this paper. The proposed RFM parameter optimization method can resolve the ill-posed problem by removing all of the unnecessary parameters based on scatter matrix and elimination transformation strategies. The performances of conventional ridge estimation and the proposed method are evaluated with control and check grids generated from Satellites d'observation de la Terre (SPOT-5) high-resolution satellite data. Experimental results show that the precision of the proposed method, with about 35 essential parameters, is 10% to 20% higher than that of the conventional model with all 78 parameters. Moreover, the ill-posed problem is effectively alleviated by the proposed method, and thus, the stability of the estimated parameters is significantly improved.**

***Index Terms*—Elimination transformation, high-resolution satellite (HRS) imagery, ill-posed problem, rational function model (RFM), ridge estimation, scatter matrix.**

I. Introduction

HIGH-RESOLUTION satellite (HRS) imagery has already been widely used in photogrammetry and remote sensing applications, such as land source monitoring, stereo mapping, and orthophotograph generation. However, owing to the dynamic nature of pushbroom sensors, the ephemerides and attitudes of satellite sensors are functions of time. The rigorous physical sensor model of satellite imagery is extremely complex and is very difficult to implement in digital photogrammetric workstations. Moreover, rigorous physical sensor models differ from each other among different satellite sensors, thereby causing specific problems for the automatic processing of satellite imagery. The corresponding physical sensor model has to be developed if a new pushbroom sensor is launched.

For the aforementioned disadvantages, replacing a rigorous physical sensor model by a generalized sensor model, which is independent of sensors, is necessary. The generalized model must be mathematically simple and straightforward to express the geometric relationship between a ground point and its corresponding image point.

A rational function model (RFM) is the ratio of two cubic polynomials with 80 rational polynomial coefficients (RPCs) which can describe the geometric relationship between a normalized object point and its image coordinates [1], [2]. Usually, two of the 80 coefficients are set to be 1.0, and there is subsequently a total of 78 parameters. RFM is independent of sensors, mathematically simple, and computationally fast.

There have been many achievements related to the accuracy of RFMs versus rigorous physical sensor models. Tao and Hu proposed the iterative and direct least squares solutions of RFMs under terrain-dependent and terrain-independent computation scenarios and demonstrated that RFMs can fit rigorous physical sensor models with high accuracy for both aerial photograph and SPOT data [1]. The "terrain-independent" scheme was adopted by Grodecki and Dial [2] to replace the IKONOS physical sensor model with RPCs. Experimental results by Grodecki and Dial showed that the maximum difference between the RFM and the physical sensor model is no larger than 0.04 pixel, and the root-mean-square error (rmse) is smaller than 0.01 pixel [2]. Moreover, it has already been verified that the RFM can achieve accuracy similar to that of the rigorous physical sensor model by several spaceborne sensors, such as QuickBird [3], Indian Resource Satellite-P6 [4], etc. Martha *et al.* observed that RPCs alone without ground control points (GCPs) are sufficient for the volume estimation in objective change detection [5].

The RPCs provided by satellite imagery vendors are usually derived without ground control information. The inherent biases of satellite orbit and attitude are introduced into the RPCs and thus will influence the absolute accuracy of georeferencing. There are many successful solutions to reducing the error of georeferencing by image-space correction models, such as affine transformation [3] and second-order polynomial transformation [6], [7], together with using various numbers of GCPs [8]–[10], or digital elevation models [11]. A generic method was used by Xiong and Zhang to refine the RPCs with GCPs [12] and in bundle block adjustment [13]. Achievements in the literature show that RFM can usually achieve accuracy similar to that of the rigorous physical sensor model if the proper GCPs are available.

However, it is known that the simultaneous determination of the 78 coefficients of RFM is an ill-posed problem, so the ridge estimation strategy is usually adopted to obtain reasonable RPC solutions [1]. However, the automatic determination of the optimal regularization parameter of ridge estimation is very difficult to obtain [1]. Typically, many

Manuscript received January 19, 2011; revised June 2, 2011 and September 14, 2011; accepted October 15, 2011. Date of publication December 26, 2011; date of current version June 20, 2012. This work was supported in part by the National Natural Science Foundation of China under Grants 41071233 and 41171292 and in part by the National Key Technology Research and Development Program under Grant 2011BAH12B05.

Y. Zhang, Y. Lu, and X. Huang are with the School of Remote Sensing and Information Engineering, Wuhan University, Wuhan 430079, China (e-mail: zhangyj@whu.edu.cn; yangguang2936@163.com; huangxu.chess@163.com).

L. Wang was with the School of Remote Sensing and Information Engineering, Wuhan University, Wuhan 430079, China. She is now with the Third Surveying and Mapping Institute, Sichuan Bureau of Surveying and Mapping, Chengdu 610500, China (e-mail: qileigirl@yahoo.com.cn).

Color versions of one or more of the figures in this paper are available online at http://ieeexplore.ieee.org.

Digital Object Identifier 10.1109/TGRS.2011.2174797

potential solutions are computed with different regularization values, and then, the best one is selected by the L-curve-based method [14], [15].

A new RFM parameter estimation method based on scatter matrix and stepwise regression is proposed in this paper. The conventional strategy of RFM parameter computation is presented in the next section. Then, the new model of RFM parameter estimation based on scatter matrix and stepwise regression is discussed in detail. Two data sets are used for experiments in Section IV, and finally, the conclusions are outlined in Section V.

II. Conventional Strategy of RFM Parameter Computation

The RFM uses the ratio of two cubic polynomials to represent the rigorous geometric sensor model of satellite imagery. To improve the numerical stability, both the image-space and object-space coordinates are normalized into the range of $(-1, +1)$ [2]. The model has the following general form as presented by Grodecki and Dial [2]:

$$\begin{cases} S_r = \frac{Num_L(P,L,H)}{Den_L(P,L,H)} \\ S_c = \frac{Num_S(P,L,H)}{Den_S(P,L,H)} \end{cases} \tag{1}$$

where (S_r, S_c) and (P, L, H) are the normalized coordinates of the image-space and object-space points, respectively. The four polynomials $Num_L(P, L, H)$, $Den_L(P, L, H)$, $Num_S(P, L, H)$, and $Den_S(P, L, H)$ have the following general form [2]:

$$\begin{aligned} &Num_L(P,L,H) \\ &\quad = a_0 + a_1L + a_2P + a_3H + a_4LP + a_5LH + a_6PH \\ &\qquad + a_7L^2 + a_8P^2 + a_9H^2 + a_{10}PLH + a_{11}L^3 \\ &\qquad + a_{12}LP^2 + a_{13}LH^2 + a_{14}L^2P + a_{15}P^3 \\ &\qquad + a_{16}PH^2 + a_{17}L^2H + a_{18}P^2H + a_{19}H^3 \\ &Den_L(P,L,H) \\ &\quad = 1 + b_1L + b_2P + b_3H + b_4LP + b_5LH + b_6PH \\ &\qquad + b_7L^2 + b_8P^2 + b_9H^2 + b_{10}PLH + b_{11}L^3 \\ &\qquad + b_{12}LP^2 + b_{13}LH^2 + b_{14}L^2P + b_{15}P^3 \\ &\qquad + b_{16}PH^2 + b_{17}L^2H + b_{18}P^2H + b_{19}H^3 \\ &Num_S(P,L,H) \\ &\quad = c_0 + c_1L + c_2P + c_3H + c_4LP + c_5LH + c_6PH \\ &\qquad + c_7L^2 + c_8P^2 + c_9H^2 + c_{10}PLH + c_{11}L^3 \\ &\qquad + c_{12}LP^2 + c_{13}LH^2 + c_{14}L^2P + c_{15}P^3 \\ &\qquad + c_{16}PH^2 + c_{17}L^2H + c_{18}P^2H + c_{19}H^3 \\ &Den_S(P,L,H) \\ &\quad = 1 + d_1L + d_2P + d_3H + d_4LP + d_5LH + d_6PH \\ &\qquad + d_7L^2 + d_8P^2 + d_9H^2 + d_{10}PLH + d_{11}L^3 \\ &\qquad + d_{12}LP^2 + d_{13}LH^2 + d_{14}L^2P + d_{15}P^3 \\ &\qquad + d_{16}PH^2 + d_{17}L^2H + d_{18}P^2H + d_{19}H^3 \end{aligned}$$

where a_i, b_i, c_i, and d_i $(i = 0, 1, 2, \ldots, 19)$ are the coefficients of the RFM parameters with $b_0 = 1$ and $d_0 = 1$.

Equation (1) can be converted into the following linear form with n being the number of observations:

$$\begin{bmatrix} 1 & L_1 & \cdots & H_1^3 & -S_{r1}L_1 & \cdots & -S_{r1}H_1^3 \\ 1 & L_2 & \cdots & H_2^3 & -S_{r2}L_2 & \cdots & -S_{r2}H_2^3 \\ \vdots & \vdots & \vdots & \vdots & \vdots & \vdots & \vdots \\ 1 & L_n & \cdots & H_n^3 & -S_{rn}L_n & \cdots & -S_{rn}H_n^3 \end{bmatrix} \begin{pmatrix} a_0 \\ a_1 \\ \vdots \\ a_{18} \\ a_{19} \\ b_1 \\ b_2 \\ \vdots \\ b_{18} \\ b_{19} \end{pmatrix} - \begin{bmatrix} S_{r1} \\ \vdots \\ S_{rn} \end{bmatrix} = 0 \tag{2}$$

$$\begin{bmatrix} 1 & L_1 & \cdots & H_1^3 & -S_{c1}L_1 & \cdots & -S_{c1}H_1^3 \\ 1 & L_2 & \cdots & H_2^3 & -S_{c2}L_2 & \cdots & -S_{c2}H_2^3 \\ \vdots & \vdots & \vdots & \vdots & \vdots & \vdots & \vdots \\ 1 & L_n & \cdots & H_n^3 & -S_{cn}L_n & \cdots & -S_{cn}H_n^3 \end{bmatrix} \begin{pmatrix} c_0 \\ c_1 \\ \vdots \\ c_{18} \\ c_{19} \\ d_1 \\ d_2 \\ \vdots \\ d_{18} \\ d_{19} \end{pmatrix} - \begin{bmatrix} S_{c1} \\ \vdots \\ S_{cn} \end{bmatrix} = 0. \tag{3}$$

From the mathematical point of view, (2) and (3) have no relationship when solving their corresponding RPCs since they represent the along-track (line) and cross-track (sample) directions of the sensor model, respectively. The two equations can be solved independently with the same strategy. The strategy of solving (2) will be discussed in the following.

Equation (2) can be represented by the following matrix form:

$$\mathbf{G} \cdot \boldsymbol{\beta} = \mathbf{S}_r \tag{4}$$

where

$$\mathbf{S}_r = \begin{pmatrix} S_{r1} \\ S_{r2} \\ \vdots \\ S_{rn} \end{pmatrix} \qquad \mathbf{G} = \begin{pmatrix} 1 & G_{1,1} & \cdots & G_{1,38} \\ 1 & G_{2,1} & \cdots & G_{2,38} \\ \vdots & \vdots & \cdots & \vdots \\ 1 & G_{n,1} & \cdots & G_{n,38} \end{pmatrix}$$

with $G_{i,j}$ $(i = 1, 2, \ldots, n;\ j = 1, 2, \ldots, 38)$ being the corresponding elements of the coefficient matrix in (2), and $\boldsymbol{\beta} = (a_0 \ \cdots \ a_{19} \ \ b_1 \ \cdots \ b_{19})^{\mathrm{T}}$.

The least squares estimation $\hat{\boldsymbol{\beta}}$ of the unknowns' vector $\boldsymbol{\beta}$ can be obtained by the following normal equation:

$$\mathbf{G}^{\mathrm{T}}\mathbf{G}\hat{\boldsymbol{\beta}} = \mathbf{G}^{\mathrm{T}}\mathbf{S}_r. \tag{5}$$

The extended form of the aforementioned normal equation can be represented as follows:

$$\begin{aligned}
&na_o + \left(\sum_{i=1}^{n} G_{i,1}\right) a_1 + \cdots + \left(\sum_{i=1}^{n} G_{i,19}\right) a_{19} \\
&\quad + \left(\sum_{i=1}^{n} G_{i,20}\right) b_1 + \cdots + \left(\sum_{i=1}^{n} G_{i,38}\right) b_{19} = \sum_{i=1}^{n} S_{ri} \\
&\left(\sum_{i=1}^{n} G_{i,1}\right) a_o + \left(\sum_{i=1}^{n} G_{i,1}^2\right) a_1 + \cdots \\
&\quad + \left(\sum_{i=1}^{n} G_{i,1}G_{i,19}\right) a_{19} + \left(\sum_{i=1}^{n} G_{i,1}G_{i,20}\right) b_1 + \cdots \\
&\quad + \left(\sum_{i=1}^{n} G_{i,1}G_{i,38}\right) b_{19} = \sum_{i=1}^{n} G_{i,1}S_{ri} \\
&\qquad \cdots \\
&\left(\sum_{i=1}^{n} G_{i,38}\right) a_o + \left(\sum_{i=1}^{n} G_{i,38}G_{i,1}\right) a_1 + \cdots \\
&\quad + \left(\sum_{i=1}^{n} G_{i,38}G_{i,19}\right) a_{19} + \left(\sum_{i=1}^{n} G_{i,38}G_{i,20}\right) b_1 + \cdots \\
&\quad + \left(\sum_{i=1}^{n} G_{i,38}^2\right) b_{19} = \sum_{i=1}^{n} G_{i,38}S_{ri}. \qquad (6)
\end{aligned}$$

It is well known that the above model is overparameterized [1], which means that not all of the 78 parameters are necessary. Usually, a biased estimation method, such as ridge estimation, is used to resolve the ill-posed problem of the normal matrix when computing RPCs. A certain real number, called the regularization parameter, is added to the diagonal elements of the normal matrix in (5) before the normal matrix is inversed. However, automatic determination of the best regularization parameter is still a difficult task.

In this paper, a new approach of RPC computation is presented. The scatter matrix and stepwise regression strategies are used to resolve the problem to be solved.

III. Optimization of RFM Parameters Based on Scatter Matrix and Stepwise Regression

Elimination transformation or sweep transformation [14] can be used to eliminate the redundant parameters of linear models and thus obtain unbiased estimation of the necessary unknown parameters. How to estimate the unknown parameters $\hat{\boldsymbol{\beta}}$ under the least squares criteria will be addressed in the following.

The first row in (6) can be converted into the following form:

$$a_o = \overline{S}_r - a_1\overline{G}_1 - \cdots - a_{19}\overline{G}_{19} - b_1\overline{G}_{20} - \cdots - b_{19}\overline{G}_{38} \qquad (7)$$

where $\overline{G}_j = (1/n)\sum_{i=1}^{n} G_{i,j}$ $(j = 1, 2, \ldots, 38)$ and $\overline{S}_r = (1/n)\sum_{i=1}^{n} S_{ri}$.

Substituting (7) into (6) except the first row, we can obtain

$$\begin{pmatrix} L_{1,1} & \cdots & L_{1,m} \\ L_{2,1} & \cdots & L_{2,m} \\ \vdots & \cdots & \vdots \\ L_{m,1} & \cdots & L_{m,m} \end{pmatrix} \begin{pmatrix} a_1 \\ \vdots \\ a_{19} \\ b_1 \\ \vdots \\ b_{19} \end{pmatrix} = \begin{pmatrix} L_{1,r} \\ L_{2,r} \\ \vdots \\ L_{m,r} \end{pmatrix} \qquad (8)$$

where $L_{j,k} = \sum_{i=1}^{n}(G_{i,j} - \overline{G}_j)(G_{i,k} - \overline{G}_k)$ $(j, k = 1, 2, \ldots, m)$, $L_{j,r} = \sum_{i=1}^{n}(G_{i,j} - \overline{G}_j)(S_{r,i} - \overline{S}_r)$ $(j = 1, 2, \ldots, m)$, and m is the number of unknowns in the above equation. Here, $m = 38$ because the unknown a_o is eliminated by substituting (7) into (6).

The $(m+1)$th-order scatter matrix can be constructed as follows:

$$\mathbf{L} = \begin{bmatrix} \mathbf{G}^{\mathrm{T}}\mathbf{G} & \mathbf{G}^{\mathrm{T}}\mathbf{S}_r \\ \mathbf{S}_r^{\mathrm{T}}\mathbf{G} & \mathbf{S}_r^{\mathrm{T}}\mathbf{S}_r \end{bmatrix} = \begin{pmatrix} L_{1,1} & \cdots & L_{1,m} & L_{1,m+1} \\ L_{2,1} & \cdots & L_{2,m} & L_{2,m+1} \\ \vdots & \cdots & \vdots & \vdots \\ L_{m,1} & \cdots & L_{m,m} & L_{m,m+1} \\ L_{m+1,1} & \cdots & L_{m+1,m} & L_{m+1,m+1} \end{pmatrix}. \qquad (9)$$

$l_{i,j}^{(0)}$, $l_{i,m+1}^{(0)}$, and $l_{m+1,m+1}^{(0)}$ are used to represent the elements of the above matrix

$$\begin{aligned}
l_{i,j}^{(0)} &= \mathbf{G}^{\mathrm{T}}\mathbf{G} \\
&= \sum_{t=1}^{n}(G_{t,i} - \overline{G}_j)(G_{t,j} - \overline{G}_j) \quad (i, j = 1, \ldots, m) \\
l_{i,m+1}^{(0)} &= \mathbf{G}^{\mathrm{T}}\mathbf{S}_r \\
&= \sum_{t=1}^{n}(G_{t,i} - \overline{G}_i)(S_{rt} - \overline{S}_r) \qquad (i = 1, \ldots, m) \\
l_{m+1,m+1}^{(0)} &= \mathbf{S}_r^{\mathrm{T}}\mathbf{S}_r = \sum_{t=1}^{n}(S_{rt} - \overline{S}_r)^2.
\end{aligned}$$

The stepwise regression strategy is adopted to select the necessary unknowns in (2). The sum of the squares of partial regression is treated as the importance measurement of a certain unknown. The unknown selection procedure is an iterative process. The initial number of unknowns is zero. In a certain iteration, the unknown with the maximum sum of squares of partial regression is selected as the potential candidate and verified by significance testing with F-distribution. The unknown is accepted into the equation if the significance value is $F_{\mathrm{in}}(1, n-t-2) \geq F_{\mathrm{out}}(1, n-t-1)$ (t is the number of accepted unknowns). Here, $F_{\mathrm{in}}(1, n-t-2)$ and $F_{\mathrm{out}}(1, n-t-1)$ are calculated by the distribution table of the F-test with significance levels α_{in} (to introduce an unknown) and α_{out} (to remove an unknown), respectively.

Note that, once there are three or more unknowns in the equation, we must test if a certain already accepted unknown should be rejected when an unknown is accepted into the equation. The iteration is terminated when no unknown can

be accepted or rejected. The detailed procedures of stepwise regression can be explained as follows.

1) Computing the sum of squares of partial regression of each unknown.

$$P_j^{(0)} = \left(l_{j,m+1}^{(0)}\right)^2 / l_{j,j}^{(0)} \qquad (j = 1, 2, \ldots, m). \tag{10}$$

Here, we assume that $P_{i1}^{(0)} = \max_{j=1,2,\ldots,m} P_j^{(0)}$ with $i1$ being the serial number of the unknown with the maximum sum of squares of partial regression and β_{i1} is the unknown corresponding to $P_{i1}^{(0)}$.

2) Verifying whether β_{i1} can be introduced into the equation.

$$F_1^{(0)} = \frac{P_{i1}^{(0)}}{Q(i1)/(n-2)} = \frac{P_{i1}^{(0)}(n-2)}{l_{m+1,m+1}^{(0)} - P_{i1}^{(0)}}. \tag{11}$$

β_{i1} is introduced into the equation if $F_1^{(0)} > F_{\text{in}}(1, n-2)$. Here, $n-2$ is the number of degrees of freedom with one unknown; $Q(i1)$ is the sum of squares of the $i1$th unknown residues. Elimination transformation is performed on the initial matrix $\mathbf{l}^{(0)}$ with $(i1, i1)$ being the pivot element, and thus, $\mathbf{L}^{(1)} = \mathbf{T}_{i1}\mathbf{L}^{(0)}$ can be obtained. Otherwise, the unknown selection process is terminated.

3) Computing the sum of squares of partial regression after t times of transformation.

Supposing that t unknowns are accepted, the matrix $\mathbf{L}^{(t)} = \mathbf{T}_{it} \cdots \mathbf{T}_{i1}\mathbf{L}^{(0)}$ can be obtained after t times of elimination transformation are applied on the initial matrix $\mathbf{L}^{(0)}$. The sum of squares of partial regression of each unknown can be computed by

$$P_i^{(t)} = \left(l_{i,m+1}^{(t)}\right)^2 \Big/ l_{i,i}^{(t)} \qquad (i = 1, 2, \ldots, m). \tag{12}$$

Here, we assume that β_{j0} is the unknown that has the maximum influence on $\mathbf{S}_r$ but has not been included in the equation.

4) Verifying whether β_{j0} can be introduced into the equation

$$F_1^{(t)} = \frac{P_{j0}^{(t)}}{Q(i1, \ldots, it, j0)/(n-t-2)} = \frac{P_{j0}^{(t)}(n-t-2)}{l_{m+1,m+1}^{(t)} - P_{j0}^{(t)}}. \tag{13}$$

β_{j0} is accepted if $F_1^{(t)} \geq F_{\text{in}}(1, n-t-2)$; then, a new matrix $\mathbf{L}^{(t+1)} = \mathbf{T}_{j0}\mathbf{L}^{(t)}$ can be obtained by elimination transformation of $\mathbf{L}^{(t)}$ with $(j0, j0)$ being the pivot element. However, the unknown selection process is terminated if $F_1^{(t)} < F_{\text{in}}(1, n-t-2)$. Here, $(n-t-2)$ is the number of degrees of freedom with t unknowns, and $Q(i1, \ldots, it, j0)$ is the sum of squares of the unknowns' residues with number $(i1, \ldots, it, j0)$.

5) Verifying whether β_{i0} should be rejected out from the equation.

As long as three or more unknowns are introduced into the equation, we must test if a certain already accepted unknown should be rejected when more unknowns are accepted into the equation. Here, we assume that β_{i0} is the unknown that has already been included in the equation and has the minimum influence on $\mathbf{S}_r$.

$$F_2^{(t)} = \frac{P_{i0}^{(t)}}{Q(i1, \ldots, it)/(n-t-1)} = \frac{P_{i0}^{(t)}(n-t-1)}{l_{m+1,m+1}^{(t)}}. \tag{14}$$

If $F_2^{(t)} \leq F_{\text{out}}(1, n-t-1)$, β_{i0} should be rejected, and a new matrix $\mathbf{L}^{(t+1)} = \mathbf{T}_{i0}\mathbf{L}^{(t)}$ can be obtained by elimination transformation on $\mathbf{L}^{(t)}$ with $(i0, i0)$ being the pivot element. Otherwise, the program returns to step 4 to verify whether more unknowns can be introduced.

After all of the essential unknowns are introduced into the equation, the optimum linear regression equation can be obtained. Supposing that h $(h \leq m)$ unknowns are introduced into the equation, the final matrix $\mathbf{L}^{(h)}$ can be obtained by h times of elimination transformation on $\mathbf{L}^{(0)}$

$$\mathbf{L}^{(h)} = \mathbf{T}_{ih} \cdots \mathbf{T}_{i1}\mathbf{L}^{(0)}. \tag{15}$$

The frontal m elements of the last column of matrix $\mathbf{L}^{(h)}$ are the final least squares solution of the unknown vector $\boldsymbol{\beta}$.

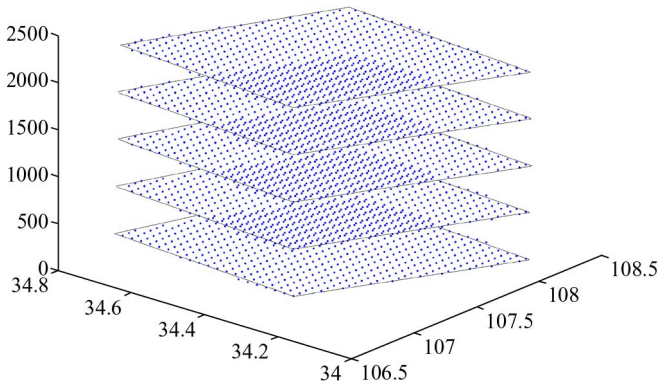

Fig. 1. Spatial grids of the first data set.

IV. Experimental Results

To verify the correctness and feasibility of the proposed approach, two experiments were performed with spatial grids generated by SPOT-5 HRS data. The two test data sets and the experimental results will be discussed in the following.

A. Test Data Sets

The first data set is generated by the rigorous sensor model of SPOT-5 HRS imagery. The original image size is 12 000 × 12 000 pixels. The elevation of the spatial grids varies from 200 to 2200 m. There are totally five layers with 500-m height interval for control and check points, as shown in Fig. 1. There are 552 image points evenly distributed in the image plane. One-half of them are used as control points, and the other half are used as check points for the experiment. A spatial ray can be determined for each image point by the projection center and its image coordinate. The corresponding spatial coordinate

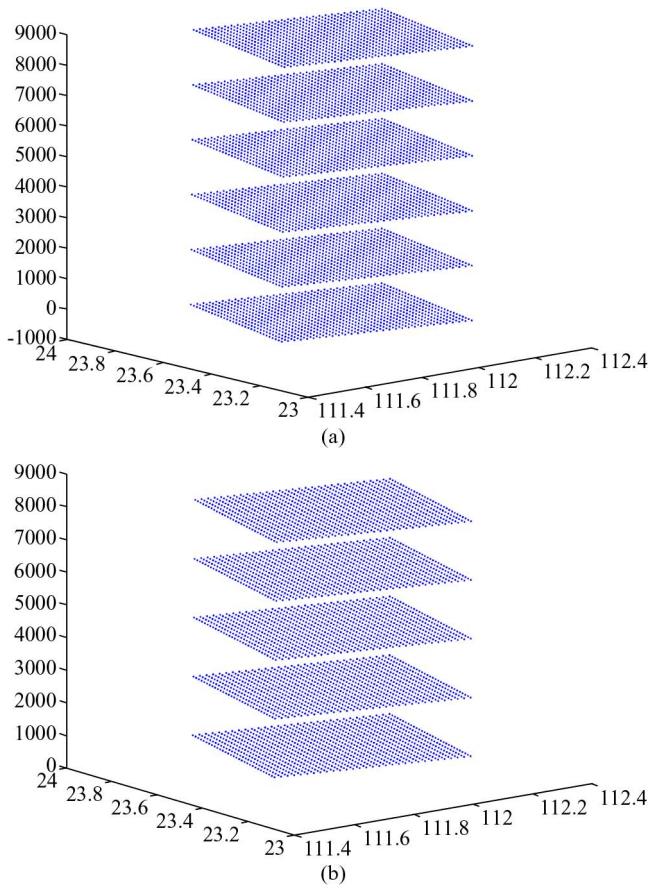

Fig. 2. Spatial grids of the second data set. Control grids are shown in (a); check grids are provided in (b).

of an image point can be calculated by the intersection between the ray and a level plane with known elevation.

The second data set is also generated from SPOT-5 HRS imagery, but only the central part (i.e., 6000 pixels) of each scanner line is used for the experiment, as shown in Fig. 2. The image size for the experiment is 6000 × 6000 pixels. The image plane is divided into regular grids with 200 × 200 pixel intervals, so there are 900 points in the image plane. The minimum and maximum elevations are 0 and 9000 m, respectively. A total of 11 layers of spatial grids is evenly distributed in the range of the elevations. The six odd layers are used as control points, and the other five even layers are used as check points for the experiment.

B. Results of Stepwise Optimization of RFM Parameters

The aforementioned two data sets are both used to compute the corresponding RFM parameters with the proposed stepwise optimization strategy. The remaining items of the original 78 RFM parameters with the two data sets are shown in Tables I and II, respectively. "Sample" and "Line" in the two tables represent the cross- and along-track directions, while "Numerator" and "Denominator" represent the numerator and denominator of the cubic polynomials, respectively. Each number in the two tables denotes the corresponding original serial number of the kept RFM parameters. When compared to the conventional ridge estimation method that computes all of the 78 parameters, only 31 and 35 of them are kept by the proposed approach.

TABLE I
ORIGINAL SERIAL NUMBER OF COMPUTED RFM PARAMETERS WITH THE FIRST DATA SET

Items		Original Serial Number of Kept Parameters										
Cross track (Sample)	Numerator	1	2	3	4	5	8	9	12	16		
	Denominator	1	2	4	5	9	13					
Along track (Line)	Numerator	1	2	3	4	5	7	8	9	10	13	
	Denominator	1	2	3	5	8	12	13	15			

TABLE II
ORIGINAL SERIAL NUMBER OF COMPUTED RFM PARAMETERS WITH THE SECOND DATA SET

Items		Original Serial Number of Kept Parameters										
Cross track (Sample)	Numerator	1	2	3	4	5	8	9	10	15	16	
	Denominator	1	2	3	4	8						
Along track (Line)	Numerator	1	2	3	4	5	8	9	10	12	13	15
	Denominator	1	2	4	5	6	7	9	10	13	15	16

The computing efficiency of the proposed method is also superior to that of the conventional ridge estimation based on the L-curve method. The proposed method only requires about 30 iterations to obtain the optimal solution, while the L-curve method usually requires more than 200 iterations [15].

The precision of the calculated RFM parameters directly influences the possible applications of HRS imagery. In order to evaluate whether the precision of the computed RFM parameters by the proposed method is comparable to that by the conventional method, the error statistics of the calculated RFM parameters for the two methods are compared with each other. As shown in Tables III and IV, the precision of the computed RFM parameters by the proposed method is 10% to 20% higher than those of the conventional method, regardless of the maximum/minimum residues or the rmses. Introducing more parameters than those listed in Tables III and IV contributes very little to further improvement. These results show that the proposed method is more accurate and advantageous than the conventional method.

However, the precision of the RFM of the second data set is higher than that of the first data set. For example, the maximum residue of the first data set is about 0.15 pixel, while it is smaller than 0.05 pixel for the second data set, which occurs because the first data set has a wider field of view and fewer control points compared to the second data set. It is reasonable to conclude that, the more control points there are, the narrower the field of view and therefore the higher the precision of the RFM. Furthermore, the rmses of the along-track (line) direction of both data sets are larger than those of the cross-track (sample)

TABLE III
PRECISION OF RFM COMPUTATION WITH THE FIRST DATA SET (PIXELS)

Statistic items		Conventional ridge estimation		The proposed method	
		Control points	Check points	Control points	Check points
Cross track (Sample)	Maximum residues	-0.098076	-0.088593	-0.087532	-0.081826
	Root mean square error	0.026913	0.02748	0.025012	0.025061
Along track (Line)	Maximum residues	-0.151241	-0.162753	-0.105563	-0.105429
	Root mean square error	0.039013	0.043961	0.033503	0.036324

TABLE IV
PRECISION OF RFM COMPUTATION WITH THE SECOND DATA SET (PIXELS)

Statistic items		Conventional ridge estimation		The proposed method	
		Control points	Check points	Control points	Check points
Cross track (Sample)	Maximum residues	0.023898	0.023858	0.021381	0.021217
	Root mean square error	0.008693	0.008693	0.006840	0.006845
Along track (Line)	Maximum residues	0.045523	0.045438	-0.040221	-0.040232
	Root mean square error	0.024139	0.024139	0.020017	0.020021

TABLE V
CONDITION INDECES OF NORMAL MATRICES WITH THE FIRST AND SECOND DATASETS

Statistic items	The first dataset		The second dataset	
	Cross track (Sample)	Along tract (Line)	Cross track (Sample)	Along tract (Line)
Original RFM	4.30E+11	8.07E+11	4.16E+12	1.70E+11
Conventional ridge estimation	68899163	66657478	92781219	92617117
The proposed method	39	216	2071	132

direction, which coincides with the fact that the major error of the SPOT-5 imagery exists in the along-track direction.

The condition index is a common criterion to evaluate the status and stability of the normal matrix. The condition indices of the normal matrices with the two data sets is shown in Tables V. It can be seen that the condition index of the original normal matrix is on the $E + 11$ level, while it is on the $E + 7$ level for ridge estimation. However, after all of the insignificant RFM parameters have been rejected by the proposed method, the condition index of the normal matrix is in the range of 100–2000. It shows that the proposed method significantly decreases the condition index and thus improves the stability of the normal matrix.

V. CONCLUSION AND DISCUSSIONS

A novel method for automatic RFM parameter optimization by stepwise selection of the necessary parameters based on scatter matrix and elimination transformation has been proposed. The proposed method can fit the rigorous sensor model of HRS imagery with the least essential parameters, and thus, the ill-posed problem of RFM parameter estimation caused by overparameterization is significantly alleviated.

The experimental results show that 10% to 20% higher precision can be obtained by the proposed method with only about 35 essential parameters compared to the conventional ridge estimation with its 78 parameters. The achieved rmses of the proposed method with the first data set are both about 0.025 pixel and 0.036 pixel for the cross- and along-track directions, respectively. However, the rmses with the second data set are both about 0.007 pixel and 0.020 pixel for the cross- and along-track directions, respectively, which was caused by the first data set having a wider field of view and fewer control points.

The condition index of the normal matrix to estimate the RFM parameters with the proposed method is usually smaller

than 2000, which means that the ill-posed problem of the normal matrix is also significantly alleviated.

However, although the rmses of the proposed method and the conventional ridge estimation are both satisfying, one can see that the rmses of the along-track direction are about two times of those of the cross-track direction for both methods, indicating that there are still systematic residues in the along-track direction. The reason for these residues is that the geometries in the along- and cross-track directions are different (i.e., perspective projection in the cross-track direction and close to parallel projection in the along-track direction). Further investigation is planned to achieve more consistent results against the rigorous sensor model.

ACKNOWLEDGMENT

The authors would like to thank the anonymous reviewers and members of the editorial team for the comments and contributions.

REFERENCES

[1] C. V. Tao and Y. Hu, "A comprehensive study on the rational function model for photogrammetric processing," *Photogramm. Eng. Remote Sens.*, vol. 67, no. 12, pp. 1347–1357, Dec. 2001.
[2] J. Grodecki and G. Dial, "Block adjustment of high-resolution satellite images described by rational functions," *Photogramm. Eng. Remote Sens.*, vol. 69, no. 1, pp. 59–68, Jan. 2003.
[3] C. S. Fraser and H. B. Hanley, "Bias-compensated RPCs for sensor orientation of high-resolution satellite imagery," *Photogramm. Eng. Remote Sens.*, vol. 71, no. 8, pp. 909–915, Aug. 2005.
[4] V. Nagasubramanian, P. V. Radhadevi, R. Ramachandran, and R. Krishnan, "Rational function model for sensor orientation of IRS-P6 LISS-4 imagery," *Photogramm. Rec.*, vol. 22, no. 120, pp. 309–320, Dec. 2007.
[5] T. R. Martha, N. Kerle, V. Jetten, C. J. van Westen, and K. V. Kumar, "Landslide volumetric analysis using Cartosat-1-derived DEMs," *IEEE Geosci. Remote Sens. Lett.*, vol. 7, no. 3, pp. 582–586, Jul. 2010.
[6] X. H. Tong, S. J. Liu, and Q. H. Weng, "Bias-corrected rational polynomial coefficients for high accuracy geo-positioning of QuickBird stereo imagery," *ISPRS J. Photogramm. Remote Sens.*, vol. 65, no. 2, pp. 218–226, Mar. 2010.
[7] X. H. Tong, S. J. Liu, and Q. H. Weng, "Geometric processing of QuickBird stereo imageries for urban land use mapping: A case study in Shanghai, China," *IEEE J. Sel. Topics Appl. Earth Obs. Remote Sens.*, vol. 2, no. 2, pp. 61–66, Jun. 2009.
[8] C. S. Fraser and H. B. Hanley, "Bias compensation in rational functions for IKONOS satellite imagery," *Photogramm. Eng. Remote Sens.*, vol. 69, no. 1, pp. 53–57, Jan. 2003.
[9] C. S. Fraser, G. Dial, and J. Grodecki, "Sensor orientation via RPCs," *ISPRS J. Photogramm. Remote Sens.*, vol. 60, no. 3, pp. 182–194, May 2006.
[10] J. Wang, K. Di, and R. Li, "Evaluation and improvement of geopositioning accuracy of IKONOS stereo imagery," *ASCE J. Surveying Eng.*, vol. 131, no. 2, pp. 35–42, May 2005.
[11] T. A. Teo, L. C. Chen, C. L. Liu, Y. C. Tung, and W. Y. Wu, "DEM-aided block adjustment for satellite images with weak convergence geometry," *IEEE Trans. Geosci. Remote Sens.*, vol. 48, no. 4, pp. 1907–1918, Apr. 2010.
[12] Z. Xiong and Y. Zhang, "A generic method for RPC refinement using ground control information," *Photogramm. Eng. Remote Sens.*, vol. 75, no. 9, pp. 1083–1092, Sep. 2009.
[13] Z. Xiong and Y. Zhang, "Bundle adjustment with rational polynomial camera models based on generic method," *IEEE Trans. Geosci. Remote Sens.*, vol. 49, no. 1, pp. 190–202, Jan. 2011.
[14] A. Neumaier, "Solving ill-conditioned and singular linear systems: A tutorial on regularization," *SIAM Rev.*, vol. 40, no. 3, pp. 636–666, 1998.
[15] Y. T. Zhu, L. Sun, and H. L. Xu, "L-curve based Tikhonov's regularization method for determining relaxation modulus from creep test," *J. Appl. Mech.*, vol. 78, no. 3, p. 031002, May 2011, 7 pages.

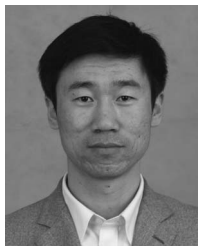

Yongjun Zhang was born in 1975. He received the B.S., M.S., and Ph.D. degrees from Wuhan University, Wuhan, China, in 1997, 2000, and 2002, respectively.

He is currently a Professor of photogrammetry and remote sensing with the School of Remote Sensing and Information Engineering, Wuhan University. His research interests include space, aerial, and low-attitude photogrammetry, image matching, combined bundle adjustment with multisource data sets, 3-D city reconstruction, and industrial inspection.

Yihui Lu was born in 1987. She received the B.S. degree from Shandong University, Jinan, China, in 2009. She is currently working toward the Ph.D. degree in the School of Remote Sensing and Information Engineering, Wuhan University, Wuhan, China.

Her research interests include satellite remote sensing and image matching.

Lei Wang was born in 1985. She received the B.S. degree from Chongqing University, Chongqing, China, in 2008 and the M.S. degree from Wuhan University, Wuhan, China, in 2010.

She is currently with the Third Surveying and Mapping Institute, Sichuan Bureau of Surveying and Mapping, Chengdu, China.

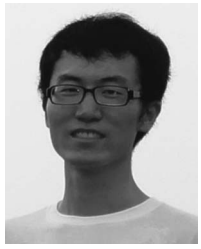

Xu Huang was born in 1987. He received the B.S. degree from Wuhan University, Wuhan, China, in 2010, where he is currently working toward the Ph.D. degree in the School of Remote Sensing and Information Engineering.

His research interests include computer vision, space/low-attitude photogrammetry, and 3-D reconstruction.